Polymer 50 (2009) 1062–1066

Contents lists available at ScienceDirect

Polymer

journal homepage: www.elsevier.com/locate/polymer

Monte-Carlo modeling of dense polymer melts near nanoparticles

Yves Termonia

NanoTechnology Core Group, Central Research and Development, Experimental Station, E.I. du Pont de Nemours, Inc., P.O. Box 80304, Wilmington, DE 19880-0304, USA

ARTICLE INFO

Article history:
Received 24 September 2008
Received in revised form
16 December 2008
Accepted 17 December 2008
Available online 24 December 2008

Keywords:
Monte-Carlo
Modeling
Nanoparticle

ABSTRACT

Using Monte-Carlo techniques, we study polymer chain conformations near nanoparticles for dense melts of high molecular weight. Our results indicate the presence of a thin interfacial region (1–2 nm in thickness) within which polymer segments orient tangentially to the particle surface causing a stretching and widening of the chain ellipsoid. That region is also characterized by an accumulation of chain ends and a decrease in polymer density. Nanoparticles also affect polymer properties far away into the bulk. Thus, at small particle radius, we observe an overall swelling of the polymer chains when the distance between the centers of mass of nearest-neighbor particles becomes smaller than the radius of gyration of the chains.

1. Introduction

It is now well accepted that the incorporation of nanoparticles into polymeric matrices can lead to a novel range of materials with properties unsurpassed in conventional composite systems. A full grasp of the potential of these nanomaterials is however still in its infancy in spite of the numerous modeling approaches that have been proposed within the last decade. For an excellent up-to-date review, see Ref. [1]. Although we have made progress towards an understanding of the relationship between the composite properties and the individual characteristics of polymer and particles [2], little is known however about the changes in structure and dynamics of the bulk polymer brought upon by the presence of the inclusions.

The issue of polymer chain configurations around nanoparticles has received a lot of attention. Off-lattice simulations using Monte-Carlo (MC) [3–5] and molecular dynamics [6,7] techniques have indicated an ordering of the polymeric units into densely packed shells around the inclusions. Bead–spring models [8–11] using high coordination lattices also revealed that the ellipsoidal chains orient their large semi-axis in a direction tangential to the filler surface. Rotational isomeric state (RIS) studies for single "phantom" chains [12–14] have shown a decrease in chain dimension for large particles and short chains and a considerable increase for small particles and long chains. These predictions however were not confirmed by later MC investigations of realistically dense polymer melts [3,16] which indicated a decrease in chain dimensions in both cases, *i.e.* when the particles are much larger or slightly smaller than the radius of gyration of the chains.

In view of their extensive computer time requirements, all previous investigations have been restricted to relatively short chains and moderate to low densities. Long chain polymers on the other hand have been reported to be particularly sensitive to the presence of nanoinclusions and the changes in entanglement density around inclusions still remain an unresolved issue in polymer physics [17,18]. In the present work, we focus on very dense polymer melts with chain lengths typical of those for commercial polymers. In our approach, the chains are simulated on a simple cubic lattice and equilibrated using very efficient computer algorithms based on the work of Pakula et al. [19,20].

2. Model

In our approach, the array of polymer chains and spherical particles is generated on a simple cubic lattice with periodic boundary conditions. The unit lattice length equals that of a statistical segment [21] for the chains. For polyethylene, the segment has length ~1 nm and molecular weight ~140, which corresponds to ~10 CH_2 groups. The density ρ of the chains in the melt equals 0.92. For simplicity, the present study focuses only on entropic constraints and consideration of various adsorption potentials between the polymer and the nanoparticles is relegated to future work.

Filling the lattice with particles and a dense melt of long polymer chains is not a trivial task. In our approach, the lattice sites are first divided into cubic blocks of two types:

(i) blocks representing the polymer melt and (ii) blocks accounting for the particles. The blocks for the two types are

E-mail address: yves.termonia@usa.dupont.com

0032-3861/$ – see front matter © 2008 Elsevier Ltd. All rights reserved.
doi:10.1016/j.polymer.2008.12.032

selected at random and according to the volume fraction of the particles. Blocks of the first type contain the chains in a fully ordered and folded configuration together with vacancies at a volume fraction $1-\rho$. (Herman's orientation function for the segments along the chains approximately equals +0.5.) Blocks of the second type are entirely filled in with vacancies and their overall volume fraction equals the particle volume fraction V_p. Before the start of the simulations, we also choose the location of the centers of the future particles of radius r_p. As equilibration is initiated, vacancies moving into these centers become immobilized and they turn into seeding sites for the growth of a particle. Growth occurs through the addition of vacancies moving into nearest-neighbor sites which then in turn become seeding sites. And so on and so forth until all the lattice sites within a radius r_p of the original centers have been assigned as particle sites. Upon completion of that process, equilibration of the chains continues while all the particle sites remain frozen in place and averages of all the quantities of interest are being taken.

Chain equilibration is performed using elementary moves of two types. The first set of moves (Fig. 1) takes advantage of the presence of unoccupied lattice sites (vacancies) and involves:

(i) Elementary rotations of a kink (a), crankshaft (b) or chain end (c).

Crankshafts are not allowed to rotate more than 90 degrees in order to prevent crossing of chains. Non-crossability of chains has been found critical for observing a transition from Rouse to reptation dynamics [22,23].

(ii) Slithering motion of a crankshaft leading to position exchange (d) or chain-end extension (e).

The second set of moves (Fig. 2) involves exchange of crankshafts [19,20] between two chain strands at adjacent positions. In Fig. 2a, chain **1** loses a crankshaft whereas chain **2** gains one, leading to changes in chain length for both chains. In order to conserve chain length, a loop is then initiated in which the next exchange is made to occur between a crankshaft in chain **2** chosen at random and an adjacent segment along a third chain strand, see Fig. 2b. And so on and so forth. The loop closes when chain **1** regains its lost crankshaft, as illustrated in Fig. 2a and b.

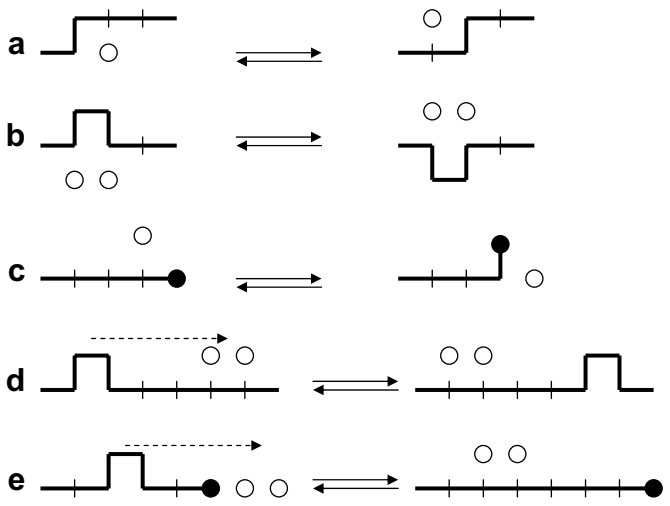

Fig. 1. Elementary moves involving vacancies (○). Moves (a), (b) and (c) lead to rotations of a kink, crankshaft and chain-end (●), respectively. Moves (d) and (e) translate a crankshaft over a chain contour leading to position exchange (d) or chain-end extension (e). All the moves are illustrated for a 2-d lattice. In a 3-d lattice, the crankshaft (move b) is not allowed to rotate more than 90 degrees in order to prevent crossing of chains (see text).

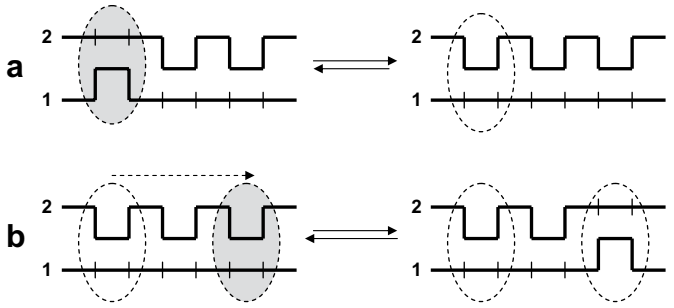

Fig. 2. Elementary moves involving exchanges of crankshaft segments between two chain strands at adjacent positions. Move (a) is for a crankshaft in chain **1** adjacent to a single segment in chain **2**. The move leads to elongation of chain **2** and shortening of chain **1**. In scheme (b), a crankshaft is selected at random along **2** and exchanged with an adjacent segment in **1**. For the short sequence illustrated in (a) + (b), chain length is restored.

In our approach, the various moves in Figs. 1 and 2 are executed sequentially. For each type of move, the lattice is swept in its entirety during which a site and its local configuration of neighbors are picked at random. If the configuration permits, the move is executed; if not, it is rejected. It is important to stress that, in order to ensure that the sequence of moves is commutative, all the lattice are visited at random and only once for each type of move [24]. Although this may not be important for static equilibrium properties, it is crucial for a study of dynamics to be presented in a forthcoming publication. Throughout the simulations, we have also verified that our process obeys detailed balance, *i.e.* reversibility for each of the moves depicted in Figs. 1 and 2. The latter is a necessary condition for thermodynamic equilibrium.

During equilibration, ensemble averages for the various chain characteristics are calculated. These include the average end-to-end vector length R_e and the gyration tensor for a chain.

$$G_{ij} = (1/N)\sum_{k=1}^{N}\left(X_k^i - X_i^{CM}\right)\left(X_j^k - X_j^{CM}\right) \tag{1}$$

in which $X^k = \{X_1^k, X_2^k, X_3^k\}$ is the position vector of polymer site k and the index CM refers the chain center of mass. We also evaluate [8,25]

$$\langle \mathrm{Tr}\mathbf{G}\rangle = \langle\lambda_1\rangle + \langle\lambda_2\rangle + \langle\lambda_3\rangle = R_g^2 \tag{2}$$

in which $\langle\lambda_1\rangle$ is the system average largest eigenvalue of $\mathbf{G}$ and R_g is the average radius of gyration.

Equilibrium is considered to be achieved when steady plateau values are reached for R_e, R_g and $\langle\lambda_i\rangle$ ($i=1,3$). For chains of length $N=600$, this was obtained after a time $t_{eq}\approx 5\times10^5$ (in units of attempted moves per lattice site). We found that t_{eq} typically increases as $\sim N^2$. Once equilibrium is reached, the simulation continues and the quantities of interest are averaged over the entire lattice and over up to 100 realizations taken at every $\Delta t = 3\times10^3$ time intervals. For simplicity, the particles are placed in an ordered body-centered-cubic configuration and they are not allowed to move during the simulations. The results (to be presented in Section 3) are for lattices of up to $66\times66\times66$ sites and chain length $N=600$ (except for Fig. 3) together with a melt density $\rho=0.92$.

3. Results and discussion

Fig. 3 shows our model results for the chain length dependence of R_g^2 and R_e^2 for a dense polymer melt with $\rho=0.92$. The relationship is linear and follows the asymptotic ideal chain limit.

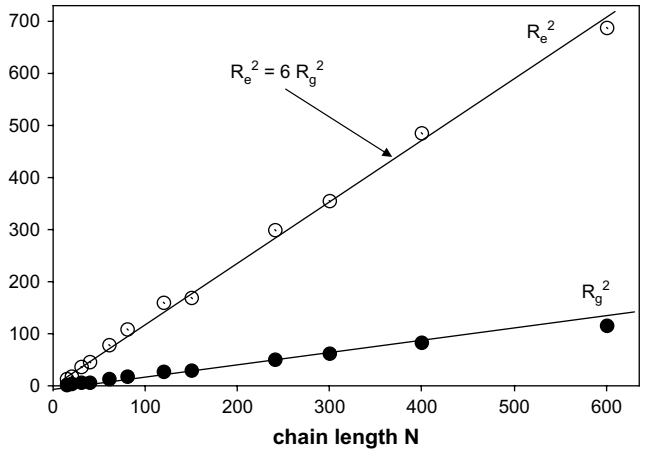

Fig. 3. Chain length dependence of the radius of gyration R_g and end-to-end distance R_e.

$$R_e^2 = 6R_g^2 \tag{3}$$

which leads to confidence in the validity of our simulations. Henceforth, unless otherwise specified, all our model results will be for long chains with $N = 600$.

Fig. 4 plots the order parameter of short chain strands of 5 consecutive units as a function of the distance of their center of mass from the surface of the closest particle. The order parameter is measured by $(3\langle\cos^2\Theta\rangle - 1)/2$ in which Θ denotes the angle between the end-to-end vector of the strand and the vector radius of the filler particle passing through the center of mass of the strand [26]. The figure is for a 10% volume fraction of particles with $r_p = 2$ nm (●) and $r_p = 15$ nm (○). The results clearly indicate the presence of an interfacial region ~1 nm in thickness within which the chains orient tangentially to the filler surface. A small overshoot in the order parameter is observed within a narrow region 1–2 nm from the filler surface, indicating a slight radial ordering of the chain segments. Our results of Fig. 4 are in agreement with those of previous off-lattice simulations [3].

Fig. 5 shows our calculated values of the polymer density as a function of the distance from the filler surface. The density has been normalized by that ($\rho = 0.92$) in the bulk. Our data again point

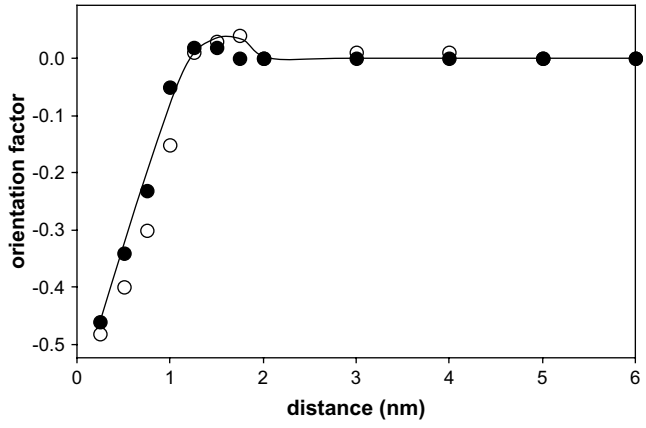

Fig. 4. Dependence of the orientation factor $(3\langle\cos^2\Theta\rangle - 1)/2$ on the distance from the closest particle for chain strands of 5 consecutive units. The distance is measured radially from the center of mass of the strand to the surface of the particle. Θ denotes the angle between the end-to-end vector of the strand and the vector radius of the filler particle through the center of mass of the strand. The figure is for a 10% volume fraction of particles with $r_p = 2$ nm (●) and $r_p = 15$ nm (○). The chain length is set at $N = 600$.

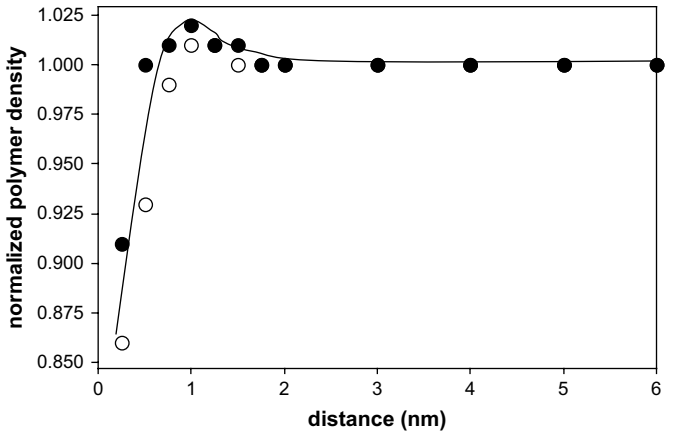

Fig. 5. Dependence of polymer density on the distance from the closed particle for chains of $N = 600$ segments. The density is normalized by the density in the bulk. Notation is the same as in Fig. 4.

to the presence of a narrow interfacial region – 1 nm thick – in which the polymer density is as much as 15% lower than that in the bulk. A small overshoot in density is observed at larger distances from the particles. Our observations are in line with those of Vacatello [3] although his results are more peculiar as they show a series of repeated minima and maxima followed by a monotonic decrease in density. That behavior was attributed to the particular arrangements assumed by the filler particles in the various simulations. Fig. 6 depicts our model predictions for the chain-end density in the near vicinity of the particles. The density is again normalized by that in the bulk. The data reveal that chain ends are located preferentially within the 1 nm-thick particle/polymer interface. This is in line with our previous observation (Fig. 5) of a higher density of vacancies within that region. The latter indeed allows for higher mobility – hence entropy – of the chain ends.

A detailed study of the eigenvalues λ_1 and λ_2 (Eq. (2)) is presented in Figs. 7 and 8 for chains of length $N = 600$ around particles of radius $r_p = 2$ nm (●) and $r_p = 15$ nm (○). The values of λ_1 and λ_2 have been normalized by λ_3. The distance is measured radially from the center of mass of a chain to the surface of the particle. At large distances from the particles, our measured eigenvalues are in the ratio $\lambda_1{:}\lambda_2{:}\lambda_3 = 12.1{:}2.8{:}1$, which is close to that expected for Gaussian chains 12.1:2.7:1. As one approaches the particles, the situation becomes entirely different. For large $r_p = 15$ nm (○), our results indicate a substantial stretching ($\lambda_1 \gg$) and widening ($\lambda_2 \gg$) of the chain ellipsoids. Our interpretation is that the latter

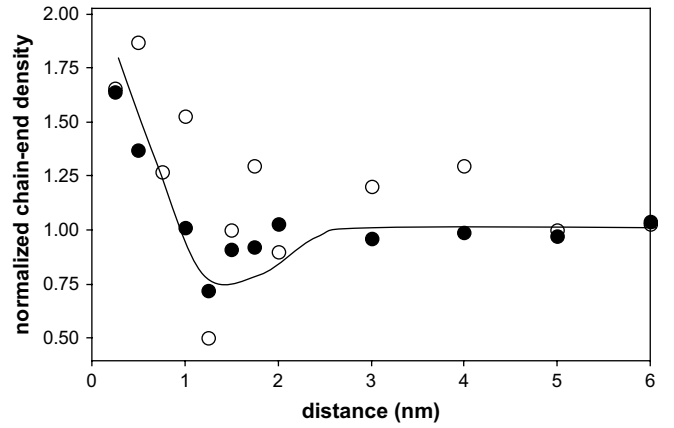

Fig. 6. Dependence of the chain-end density on the distance from the closed particle for chains of $N = 600$ segments. The density is normalized by the density in the bulk. Notation is the same as in Fig. 4.

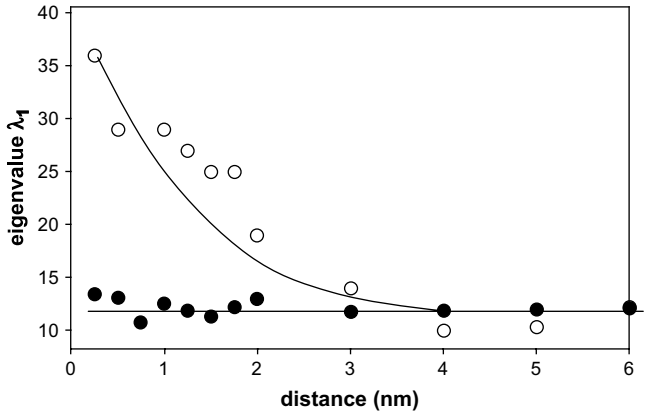

Fig. 7. Dependence of the chain eigenvalue λ_1 on the distance from the closed particle for chains of $N = 600$ segments. The eigenvalue is normalized by λ_3. The distance is measured radially from the center of mass of the whole chain to the surface of the particle. Notation is the same as in Fig. 4.

are "sacrificial" chains which loose their entropy and Gaussian character in order for the other chains to retain their properties in the bulk. At small $r_p = 2$ nm (●), all the chains remain Gaussian even at very small distances from the particles. Further analysis of the case of small r_p reveals a substantial swelling of the chains throughout the bulk, see Figs. 10 and 11.

We now turn to a model illustration of the configuration of chains closest to particles, see Fig. 9. The figure is for a dense polymer melt ($\rho = 0.92$) of chains of length $N = 600$ with 10% of particles of high radius $r_p = 15$ nm. As mentioned earlier in Section 2, the particles are arranged in a body-centered-cubic configuration. The figure only shows the two closest chains to the central particle. The illustration clearly reveals a complete wrapping of the chains around the particle. This, in turn, confirms all of our previously observed results on chain behavior at the interface with a large particle, *i.e.* (i) tangential orientation of the segments; (ii) accumulation of ends and (iii) stretching and widening of the chain ellipsoids.

Figs. 10 and 11 plot the average values of R_e^2 and R_g^2 in the bulk polymer as a function of the particle radius r_p for $N = 600$ statistical segments and two different particle volume fractions: $v_p = 10\%$ (●) and $v_p = 20\%$ (○). The figures indicate a swelling of the polymer chains at $r_p < 3$ nm and $r_p < 4$ nm for low and high volume fractions, respectively. A detailed analysis of our simulation data (see Fig. 12) reveals that, within these two regimes, the distances

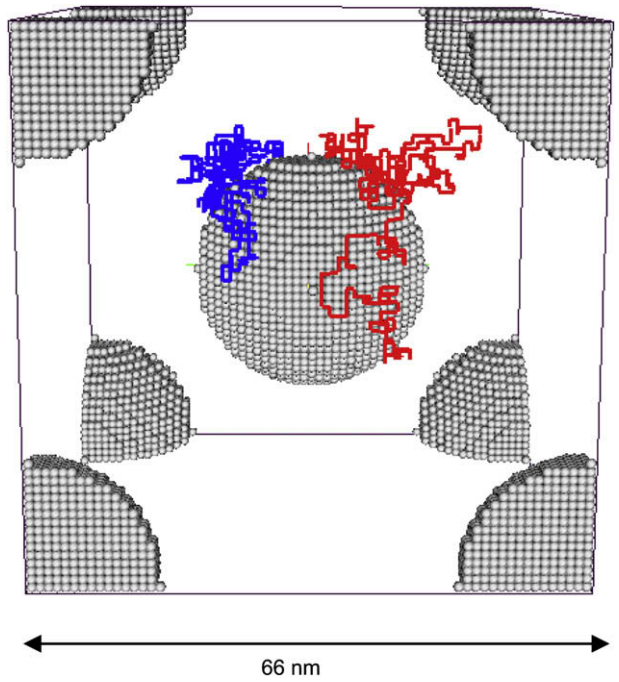

Fig. 9. Dense polymer melt ($\rho = 0.92$) of chains of length $N = 600$ with 10% of particles of high radius $r_p = 15$ nm. The particles are arranged in a body-centered-cubic configuration. The figure only shows the two closest chains to the central particle.

between the centers of mass of nearest-neighbor particles become smaller than R_g. Figs. 10 and 11 also indicate a slight chain contraction at $3 < r_p < 4$ just past the swelling regime at $v_p = 10\%$ particles but not at higher $v_p = 20\%$. The reason for that dip is not obviously clear. Further investigation of the results of Figs. 10 and 11 at low r_p reveals no associated increase in the ratios λ_1/λ_3 and λ_2/λ_3, which indicates no variation in the aspect ratio of the chain ellipsoids. Our observation of a substantial swelling of long chains $N = 600$ at small r_p is in agreement with previous rotational isomeric state (RIS) studies for single "phantom" chains [12–14]. Note however that the present work does not address the case $r_p \gg R_g$ so that the finding of chain contraction in Refs. [12–14] in that limit is not verifiable here. Our results also disagree with those of recent MC investigations [3,16] which indicated a decrease in chain dimension for all r_p R_g and $r_p \gg R_g$.

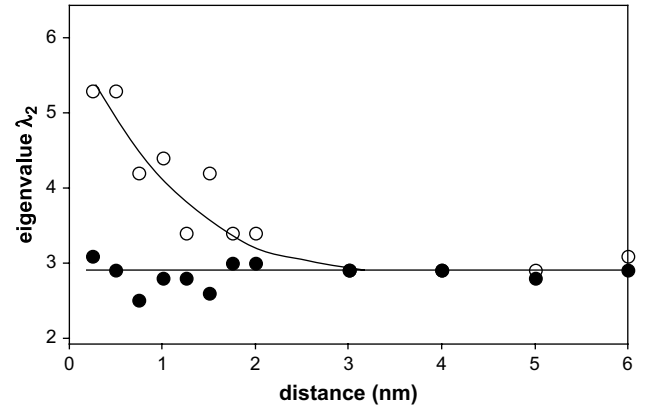

Fig. 8. Dependence of the chain eigenvalue λ_2 on the distance from the closed particle for chains of $N = 600$ segments. The eigenvalue is normalized by λ_3. The distance is measured radially from the center of mass of the whole chain to the surface of the particle. Notation is the same as in Fig. 4.

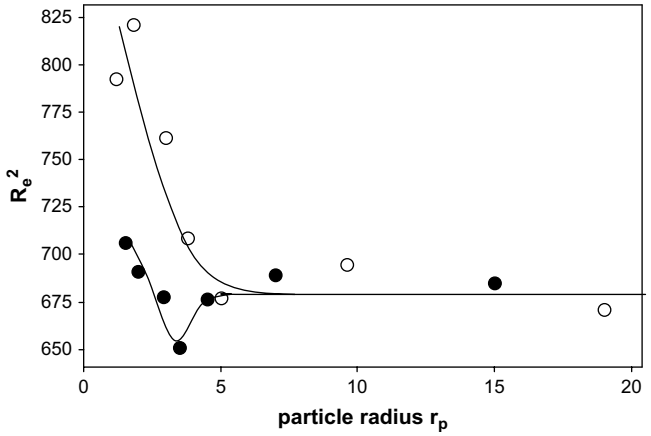

Fig. 10. Dependence of R_e^2 on particle radius at two particle volume fractions: 10% (●) and 20% (○). The data are for chains of length $N = 600$ statistical segments in the bulk.

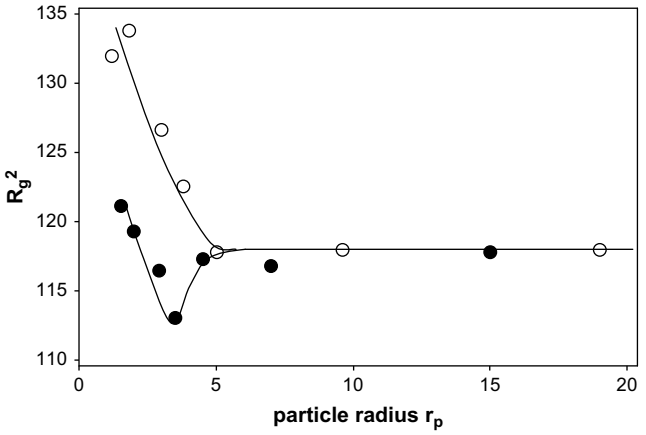

Fig. 11. Dependence of R_g^2 on particle radius. Notation is the same as for Fig. 10.

Turning to comparison with experiment, Nakatani et al. [27] have studied the dimensions of poly(dimethyl siloxane) (PDMS) chains in the presence of polysilicate particles with radius $r_p = 1$ nm. The particles were treated with trimethylsilyl to improve dispersion in the polymer. At 10% particles, they find a small contraction of short chains with $R_g = 3.4$ nm and swelling for chains of $R_g = 7.6$ nm and higher. Turning to our results of Fig. 12, the distance between the centers of mass of nearest-neighbor particles with $r_p = 1$ nm and $v_p = 0.1$ is about 5 nm. Thus, from our discussion of Fig. 11, our model for that case would predict chain swelling for $R_g > 5$ nm and contraction at smaller R_g values, in agreement with experiment. In another experimental study, Tuteja et al. [28] made well dispersed mixtures of protonated polysterene (PS) and chemically identical nanoparticles with $r_p = 2$, 2.7 and 3.6 nm. At 10% volume fraction of particles, they observe a swelling of PS chains with $R_g = 11$ at all three r_ps. Our model results of Figs. 11 and 12 for that case predict chain swelling for $r_p = 2$ and 2.7 nm but, contraction at larger $r_p = 3.6$ nm. Experimental results for shorter chains with $R_g = 5.7$ nm are in disagreement with our model. Not only do they indicate swelling at all three r_ps but, the extent of swelling is found to *decrease* with a decrease in r_p, in contrast with our results of Fig. 11. Sen et al. [29] have investigated the case of PS chains loaded with – untreated – silica nanospheres of radius $r_p = 7$ nm with volume fractions ranging from ~3 to 27%. The PS chains had R_g values ranging from ~8 nm to 22 nm, which are higher than r_p. Their results indicated no changes in polymer size, which is in contrast to our model findings and the experimental data of Refs. [27,28]. We believe that the origin of that disagreement lies in the poor dispersion quality of their samples, which is quite apparent from their TEM micrographs and would lead to a much higher effective r_p value.

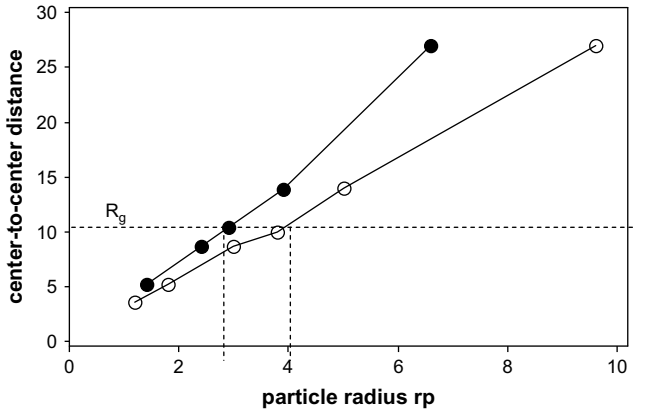

Fig. 12. Distance between the centers of mass of nearest-neighbor particles as a function of the particle radius r_p, at two difference volume fractions: 10% (●) and 20% (○). Also indicated along the *y*-axis is the R_g value for chains of length $N = 600$ statistical segments.

4. Conclusions

Using Monte-Carlo techniques originally introduced by Pakula et al. [19,20], we have studied polymer chain conformations near nanoparticles for dense melts of high molecular weight. Our results indicate the presence of a thin interfacial region within which polymer segments orient tangentially to the particle surface causing a stretching and widening of the chain ellipsoid. That region is also characterized by an accumulation of chain ends and a decrease in polymer density. These observations are in agreement with those of previous off-lattice simulations [3–5]. Nanoparticles also affect polymer properties far away into the bulk and, at small particle radius, swelling of the polymer chains is observed in our model simulations. It is proposed in Refs. [27,28] that a necessary condition for polymer swelling in the bulk is $R_g > r_p$. We find that a sufficient condition is $R_g >$ (center-to-center distance between nearest-neighbor particles), see Fig. 12.

Consideration of various adsorption potentials between the polymer and the nanoparticles will be presented in a forthcoming publication. Future work will also include a detailed study of the effect of nanoparticles on chain dynamics.

References

[1] Zheng QH, Yu AB, Lu GQ. Prog Polym Sci 2008;33:191–260.
[2] Termonia Y. Polymer 2007;48:6948–54.
[3] Vacatello M. Macromolecules 2001;34:1946–52.
[4] Vacatello M. Macromol Theory Simul 2002;11:53–7.
[5] Vacatello M. Macromol Theory Simul 2003;12:86–91.
[6] Starr FW, Schroeder TB, Glotzer SC. Macromolecules 2002;35:4481.
[7] Brown D, Marcadon V, Mele P, Alberola ND. Macromolecules 2008;41:1499–511.
[8] Ozmusul MS, Picu RC. Polymer 2002;43:4657–65.
[9] Picu RC, Ozmusul MS. J Chem Phys 2003;118:11239–48.
[10] Dionne PJ, Ozisik R, Picu CR. Macromolecules 2005;38:9351–8.
[11] Ozmusual MS, Picu CR, Sternstein SS, Kumar SK. Macromolecules 2005;38:4495–500.
[12] Kloczkowski A, Sharaf MA, Mark JE. Chem Eng Sci 1994;49:2889–97.
[13] Yuan QW, Kloczkowski A, Mark JE, Sharaf MA. J Polym Sci Part B Polym Phys 1996;34:1647–57.
[14] Sharaf MA, Mark JE. Polymer 2004;45:3943–52.
[16] Vacatello M. Macromolecules 2002;35:8191–3.
[17] Sternstein SS, Zhu AJ. Macromolecules 2002;35:7262–3.
[18] Yalcin B, Ergungor Z, Konishi Y, Cakmak M, Batur C. Polymer 2008;49:1635–50.
[19] Pakula T. Macromolecules 1987;20:679–82.
[20] Geyler S, Pakula T, Reiter J. J Chem Phys 1990;92:2676–80.
[21] Flory PJ. Statistical mechanics of chain molecules. New York: Interscience; 1969. p. 12.
[22] Kreer T, Baschnagel J, Muller M, Binder K. Macromolecules 2001;34:1105–17.
[23] Schaffer JS. J Chem Phys 1994;101:4205–13. 1995;103:761–72.
[24] Note that the number of elementary crankshaft exchanges (Fig. 2a and b) required to close the loop and conserve molecular weight often exceeds the total number of lattice sites. In such a case, the loop is momentarily interrupted to allow for the other types of moves within the sequence to proceed. During that interruption, one chain in the entire network is 3 segments (one crankshaft) shorter whereas another chain is longer by the same length.
[25] Janszen HWHM, Tervoort TA, Cifra P. Macromolecules 1996;29:5678–87.
[26] Yoon DY, Vacatello M, Smith GD. In: Binder K, editor. Monte-Carlo and molecular dynamics simulations in polymer science. New York: Oxford University Press; 1995. p. 433.
[27] Nakatani AI, Chen W, Schmidt RG, Gordon GV, Han CC. Polymer 2001;42:3713–22.
[28] Tuteja A, Duxbury PM, McKay ME. Phys Rev Lett 2008;100:077801–4.
[29] Sen S, Xie Y, Kumar SK, Yang H, Bansal A, Ho DL. Phys Rev Lett 2007;98:1283021–4.